



Proceeding of the 3rd Annual International
Conference on Information and Sciences 2023,
University of Fallujah, Iraq



<https://dx.doi.org/10.57647/j.jtap.2024.si-AICIS23.23>

Nanocomposites electrolytes based conductive polymer for electrochemical application

Fatima Mikdad Ahmed^{1,2,*} , Mohammed Kadhim Jawad¹

¹Department of Physics, College of Science, University of Baghdad, Baghdad, Iraq.

²Department of Physics, College of Science, Al-Nahrain University, Jadriya, Baghdad, Iraq.

*Corresponding author: fatima.muqdad@nahrainuniv.edu.iq.

Original Research

Published online:
15 June 2024

© The Author(s) 2024

Abstract:

Gels of PVA/PVP polymer electrolytes filled with gradient contents of SiO₂, MWCNT, and Polythiophene (PTh) were fabricated using a solution casting technique. The electrical conductivity was calculated with an impedance analyzer within the frequency range 50 Hz – 1 MHz at a temperature range 293 – 343 K and has the highest ionic conductivity with 1.5 wt.% of PTh for system E3 (PVA-PVP-KI-MWCNTs-PTh). The real dielectric constant was higher at lower frequencies. Differential scanning calorimetric thermo grams showed a single glass transition temperature, which confirms the miscibility of PVA and PVP together with the nanoparticles and conductive polymer. The highest conducting electrolytes were utilized in the fabrication and characterization of the dye-sensitized solar cell(DSSC). These DSSCs demonstrated an excellent response to a light intensity of 792 mW.cm⁻². The DSSCs with 1.5% weight percentage PTh had the best photovoltaic characteristics, with a total conversion efficiency of 3.982%, V_{oc} of 0.74 V, J_{sc} of 11.9 mA/cm, and FF of 0.453.

Keywords: FTIR; AC; Dielectric; Bulk resistance; Thermal analysis; DSSCs

1. Introduction

Conducting polymers have been extensively investigated primarily owing to their facile synthesis, exceptional conductivity, environmental durability, cost efficiency, and distinctive electrochemical redox characteristics [1]. They could be new materials with plastic solubility, processability, and flexibility with metal and semiconductor electrical and optical capabilities. Conducting polymers include carbon, hydrogen, and heteroatoms like nitrogen or sulphur. It has conjugated double bands across the polymer backbone, such as Polythiophene (PTh), polyaniline (PANI), and Polypyrrole (PPy) [2, 3]. Conducting polymers can be used as quasi-electrolytes in dye-sensitized solar cells (DSSCs) to improve their efficiency and stability. DSSCs are a form of solar cell that converts light into electricity via a dye-sensitized semiconductor by utilizing the electrolyte, dyes, and sensitization of a wide bandgap semiconductor [4]. The efficacy of the dye-sensitized solar cell (DSSC) greatly relies on the sensitizer dye and the wide bandgap materials, namely TiO₂, ZnO, and Nb₂O₅. Material TiO₂ [5] is highly preferred due to its surface's ability to resist the

continuous transfer of electrons under illumination by solar photons in the ultraviolet range. The efficiency of the solar cell is determined by important aspects such as the performance of the dye absorption spectrum, which is mounted on the surface of the TiO₂ molecule [6, 7]. They have several unique features that make them attractive for sustainable energy applications, such as their low cost, flexibility, and simplicity in fabrication. DSSC has emerged as a highly promising approach for solar energy conversion, garnering significant attention since its inception in 1991 by Grätzel [8, 9].

2. Experimental

2.1 Modification of Polythiophene (PTh)

Thiophene monomer (mTh), ferric chloride (FeCl₃), which was used as the oxidizing agent, and Chloroform (CHCl₃), with a purity of more than 98.6%, were supplied by Sigma Aldrich and Hmedia Laboratories Pvt. Ltd. Polythiophene (PTh) was synthesized by simple chemical oxidative polymerization by dissolving 3.73 g of ferric chloride (FeCl₃) in 20 mL of chloroform solvent in a beaker and stirring

for an hour. In another beaker, 0.95 mL of thiophene was dissolved in 20 mL of chloroform solvent and stirred for 30 minutes, then this solution of the thiophene was added dropwise to the mixture of ferric chloride and chloroform solvent and stirred for (5 - 6 hours) at ambient temperature, it has been noticed that the color of the solution changed to black-brown, then the solution was left to rest to the next day. The Polythiophene precipitate was collected by filtration, washed with 0.1 mL of HCl and 300 mL of ethanol several times, and dried in a hot oven at (343 K) for four hours.

2.2 Gel polymer electrolyte (GPE) preparation

The used materials in this project are PVA (M.w. approx.14000), PVP (Mw.40000), DMSO, EC, PC, KI, I₂, SiO₂, MWCNT and Polythiophene (PTh) with high purity of more than 98%. The fabrication of the samples entailed a consistent proportion of PVP, PVA(50:50), PC, EC(1:1), SiO₂ MWCNTs, 50 wt.% KI and iodine I₂ = 10% of salt wt.%, along with varying proportions of conductive polymer. First, sufficient amounts of PC, EC, and PVA were mixed in a beaker for 2 hours at 30 °C with continuous stirring. Then, PVP and KI were added to the mixture and stirred for 2 hours. Then the nanoparticles were added to the systems after obtaining the gelation. This is followed by adding conductive polymer to the mixture to get two groups of electrolytes labelled D and E. These electrolytes contain nanoparticles of 6 wt.% SiO₂ and 10 wt.% MWCNTs with various percentages of PTh, as shown in Table 1. To prevent agglomeration and aggregation, the nanoparticles and conductive polymer were added slowly to the electrolytes with continuous stirring for 1 to 3 hours. Finally, iodine (I₂) was added to the mixture while stirring continuously at room temperature for 30 minutes until gelation occurs.

Table 1. Composition of gel electrolytes system D and E.

Electrolytes Type	Conductive Polymer wt.%				
	0.5	1	1.5	2	2.5
PVA-PVP-KI-SiO ₂ -PTh	D1	D2	D3	D4	D5
PVA-PVP-KI-MWCNTs-PTh	E1	E2	E3	E4	E5

2.3 Fabrication of dye-sensitized solar cell (DSSC)

A porous TiO₂ paste is prepared using nanoparticles of 0.3 g and is blended using an agate mortar with 0.5 mL HNO₃ (pH = 1), 0.1 g of carbowax, and one drop of nonionic surfactant, TritonX-100. As shown in Fig. 1, this colloidal suspension was fabricated utilizing the doctor blade technique. A Scotch tape was employed as a masking material to confine the thickness and area of the paste on the conductive layer. Paste a thin layer onto the designated region of 0.9 cm × 0.5 cm hole using a glass rod to obtain porous TiO₂ layers of about 5 – 10 μm thickness. Later, the glass is sintered at 450 °C for an hour under the thermal furnace module. After the annealing process, when the temperature of the resulting TiO₂ nano-porous film was allowed to cool down to room temperature, the coated TiO₂/ITO glasses were immersed in ethanol solution of dye sensitizer ruthenium535-bis TBA (N₃dye) and leave for 24 hours. Excess non-adsorbed dye was then removed by rinsing the substrate with ethanol. The DSSC was prepared by sandwiching the gel electrolyte between the photoanode and platinum counter electrode. The procedure of device assembly steps is described as follows (see Fig. 2).

3. Characterization

The electrical conductivity of the samples was determined using an LCR-811G/815G impedance analyzer, which operated within the frequency range of 50 Hz to 1 MHz. The

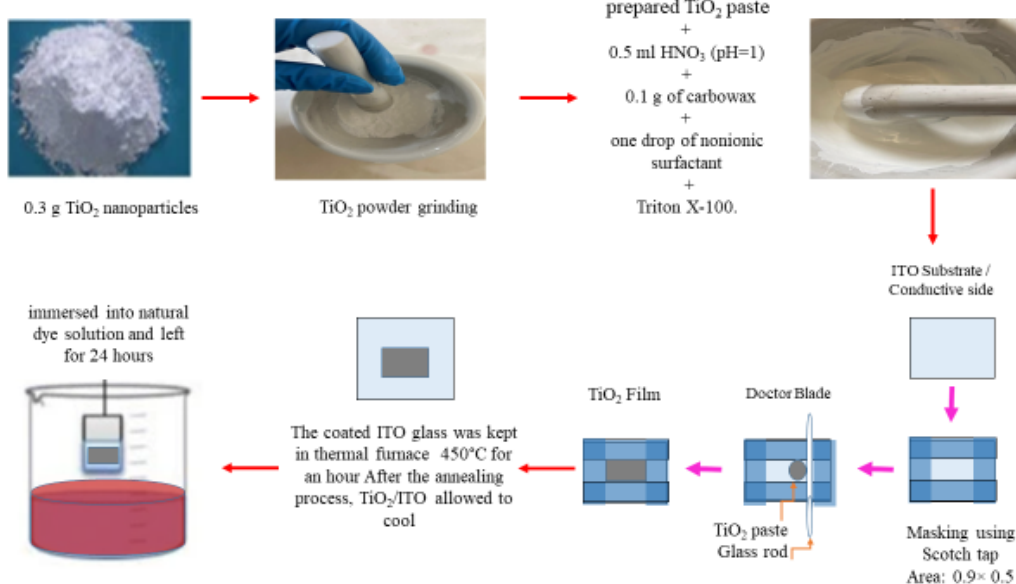


Figure 1. Experimental steps of prepared TiO₂/ITO photoanode.

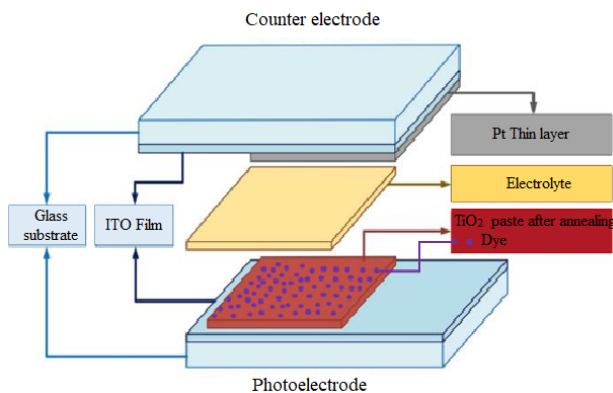


Figure 2. The assembly procedure of the ITO/TiO₂ dye/electrolyte/Pt DSSCs.

ionic conductivity (σ) of each sample was calculated using the following equation [10–14]:

$$\sigma = \frac{L}{R_b A} \quad (1)$$

where L (cm) represents the distance between the electrodes, R_b is the bulk resistance, and A (cm²) is the electrode area. The temperature of the sample was changed from the range of 293 K to 343 K. The values of the real parts of the dielectric constant (ϵ_r) were determined using the following equation [10]:

$$\epsilon_r = \frac{Z_i}{\omega C_0 (Z_r^2 + Z_i^2)} \quad (2)$$

In this equation, ω represents the angular frequency = $2\pi f$ [3, 11], C_0 is the vacuum capacitance, and Z_r and Z_i are the real and imaginary parts of the resistance, respectively. The DSC measurements of the samples were performed using the SDT Q600 V20.9 Build 20 system. Under an argon environment, the DSC thermographs were taken between 0 and 1000 °C in temperature. The DSSCs' photoelectric conversion efficiency was examined in a lab environment using a device (Keithley Model 2450) and the Xenon lamp served as the light source, and the incident light intensity was about

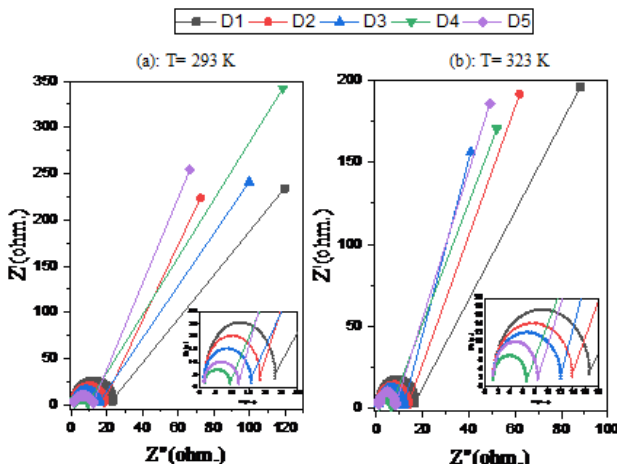


Figure 3. Nyquist plots for nanocomposite blends containing various weight percentages of PTh.

(792 mW). Starting with the current–voltage (I – V) curve, the photovoltaic properties, including the open-circuit voltage (V_{oc}), the short-circuit current density (J_{sc}), and the fill factor (FF), were evaluated on the basis of the I – V curves. For all DSSCs, the following two equations were utilized to compute the fill factor and the power conversion efficiency (η) [12–14]:

$$FF = \frac{P_m}{I_{sc} \times V_{oc}} \quad (3)$$

$$\eta = \frac{P_m}{P_{in}} = \frac{I_{sc} \cdot V_{oc} \cdot FF}{P_m} \quad (4)$$

where the incident light power entering the DSSC is represented by P_{in} (mW/cm²) and the peak power output from the DSSC is represented by P_m (mW/cm²).

4. Results and discussion

4.1 Electrical conductivity results

The Nyquist plots depict the characteristics of blend nanocomposite electrolytes with varying weight percentages: 0.5, 1, 1.5, 2, and 2.5 wt.% for PTh is presented in Figures 3 (a, and b) and 4 (a, and b), respectively. These plots were obtained at two different temperatures, particularly 293 K and 323 K, which exhibit a distinct spike-like structure at a lower frequency range. At the same time, a semicircular pattern is observed at higher frequencies. This semicircular pattern decreases gradually as both temperature and conductivity increase. This behavior can be attributed to the resistive and capacitive properties inherent in the sample [15]. The value of bulk resistance (R_b) was determined by taking the intercept of the semi-circular plot on the real axis. This value was used to calculate the ionic conductivity using Equation (1) [16]. Introducing PTh conductive polymer into the electrolyte resulted in a noticeable reduction in the bulk resistance value and, consequently, the resistivity, as evidenced by the observed changes in the Nyquist plot [17]. A decrease in the bulk resistance implies an augmentation in the ionic conductivity [18].

The conductivity of the blend electrolytes as a function of temperature and different ratios (0.5, 1, 1.5, 2, 2.5 wt.%)

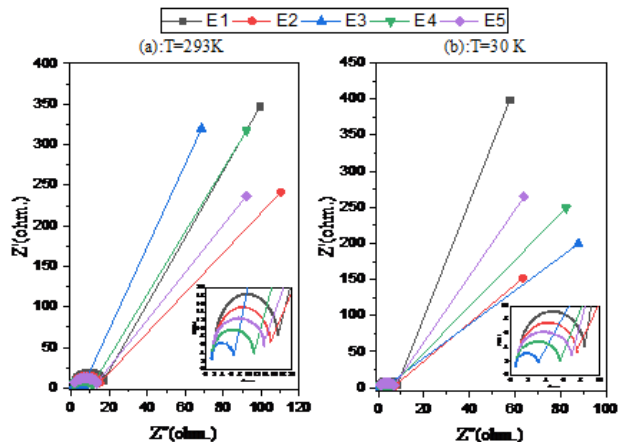


Figure 4. Nyquist plots for nanocomposite blends containing various weight percentages of PTh.

for (PTh) over the temperature range (293 - 343 K) is illustrated in Fig. 5 (a, and b). The conductance of gel polymers D and E gradually increases by increasing the temperature, obeying the Arrhenius type thermally activated [19]. Arrhenius-type behavior indicates ion transport is decoupled from polymer chain respiration via a hopping mechanism. It is evident from the plots that the bulk ionic conductivity increases as the temperature rises for all nanocomposite electrolytes, in accordance with the findings of previous studies [20]. The observed increase of the conductivity depicted in Fig. 5 can be attributed to the growth of aggregation as the concentration of PTh increases. As the concentration of PTh increases to 2 wt.%, the conductivity increases before declining, as seen in Fig. 6 (a). The electrolyte D4 has the highest conductivity with a value of 8.612×10^{-2} S/cm [21]. From Fig. 5 (b), the highest conductivity of the nanocomposites electrolyte is 1.5 wt.% of PTh (E3) is 11.167×10^{-2} (S/cm) at room temperature. The increase in conductivity can be attributed to the increase in density and/or mobility of the charge carrier [22]. According to Fig. 5, the conductivity increases as the temperature rises, which can be attributed to the great flexible polymer chains. This enhanced flexibility allows for long-distance movement of ions through coordinating sites within the polymer matrix, specifically through the segmental motion of polymer chains [23]. In Fig. 6 (a, and b), the conductivity value of the electrolytes D5 and E4 decreases, the decrease which may be due to the occurrence of agglomeration and aggregation in some areas within the paths of ions between the polymeric chains, which leads to impeding the movement of ions. This means a decrease in the mobility of ions and, thus a decrease in the conductivity values [24, 25]. The real dielectric constant (ϵ_r) signifies the capability of the dielectric material to store charges by conduction [26]. Fig. ?? illustrates the relationship between the frequency of blend nanocomposites and the variation of the real dielectric. The findings coincide with the previous study [27], showing that the real dielectric constant increases with temperature at all measured frequencies and decreases with an increase

in frequency; this decrease in dielectric constant at higher frequency is due to an increase in dielectric dispersion. This phenomenon can be attributed to the behavior of polar materials, which initially possess high real dielectric values. This can be explained by the fact that dipoles are unable to respond to rapid changes in the field at higher frequencies, coupled with the presence of polarization effects. At higher frequencies, the electric field undergoes periodic reversals so quickly because of no surplus ion diffusion occurring in the field direction. Consequently, the real dielectric decreases as the frequency increases for all the samples [28]. Furthermore, the dielectric constant (ϵ_r) indicates that the rise in the conductivity comes from an increase in the number of free mobile ions or, in simpler terms, as a fractional increase in charge. The increase in available ions is a result of ion dissociation, while the decrease is attributed to ion association [29, 30].

4.2 Differential scanning calorimeter (DSC)

The thermal phase transition behavior (T_g) of Nano-hybrid electrolytes with different contents of PTh is investigated by differential scanning calorimetry as shown in Fig. 8. It was observed that the Nano-hybrid exhibited lower glass transition (T_g) and melting (T_m) temperatures compared to the neat PVA/PVP/KI. Therefore, the decrease in T_g may be due to the increase in amorphicity of the polymer electrolyte, which in turn leads to an increase in conductivity [31]. Additionally, the (T_g) of Nano-hybrid polymer electrolytes increases as the concentration of PTh increases. This is because the conductivity of polymer electrolytes is confined to the amorphous phase above the glass-transition temperature (T_g) [32]. Therefore, the conductivity, which is coupled to the micro-Brownian motion of segments of the polymer chains above the glass-transition temperature, rises significantly with increasing amorphicity of the polymer electrolyte [33]. The DSC curve of all the samples shows two sharp endothermic peaks. The PVA/PVP/KI blend shows the T_g at 141.52 °C while the T_g of Nano-hybrid with 0.5 and 2.5 wt% of PTh appeared at 66.46 and 65.81 °C respectively for the (PVP-PVA-SiO₂-PTh) system, however

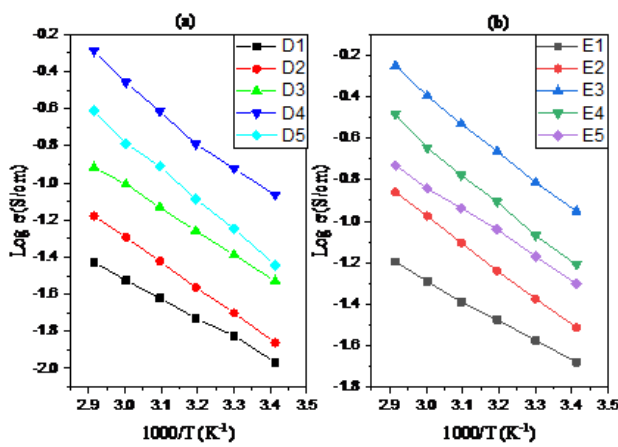


Figure 5. Ionic conductivity of the electrolytes in blended nanocomposites with (a) SiO₂ and (b) MWCNTs as a function of temperature dependent on the weight ratio of the PTh.

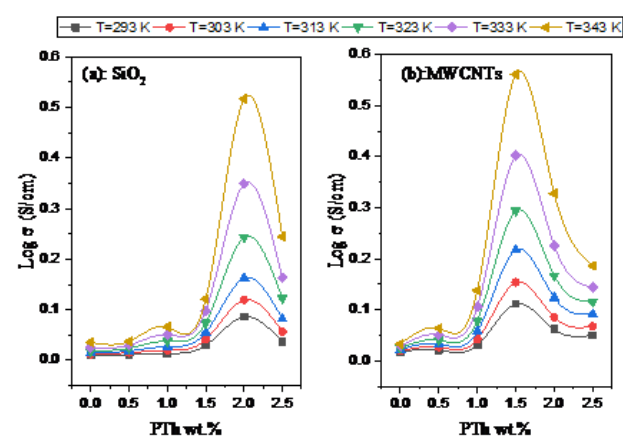


Figure 6. Ionic conductivity in nanocomposite electrolytes, (a) SiO₂, (b) MWCNTs, is dependent on the weight ratio of the PTh.

for (PVP-PVA-MWCNTs-PTh) system appeared at 67.12 and 77.54 °C respectively. The T_m values of Nano-hybrid polymer electrolyte E1 are higher than the PVA/PVP/KI blend electrolytes (Table 2) confirming the increase in their thermal stability. The melting temperature (T_m) values of these Nano-hybrid polymer electrolytes, which depend on

the concentration of conductive polymer, demonstrate that incorporating 2.5 wt.% PTh particles into the PVP-PVA-KI-MWCNTs blend matrix significantly enhance the thermal stability of the polymer blend. The changes observed in the size and shape of the endothermic peak related to T_m are also indicative of the degree of crystallinity and the strength

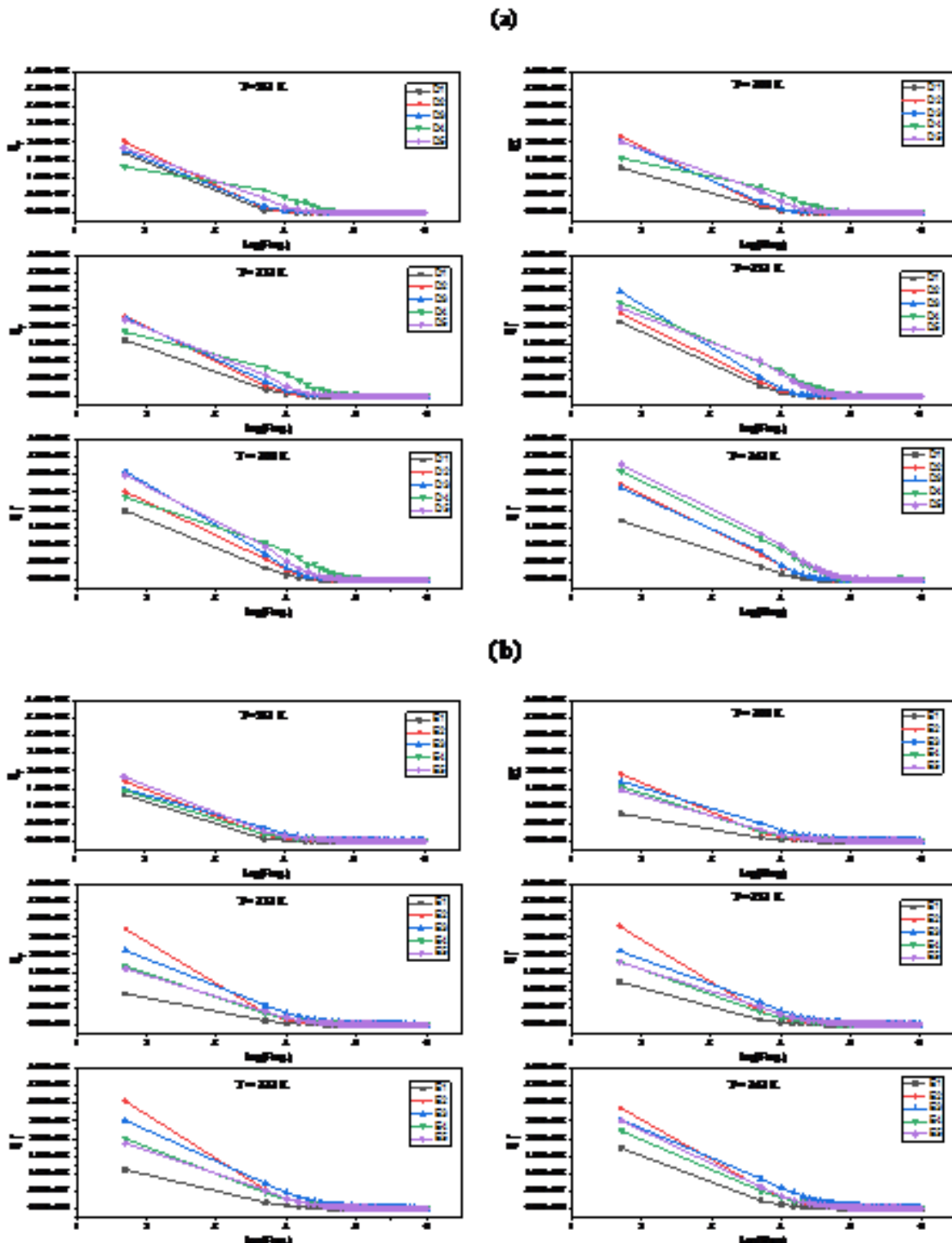


Figure 7. Dielectric constant as a function of Log frequency for blend nanocomposites at various temperatures, with various nanoparticles (a): SiO_2 , and (b): MWCNTs

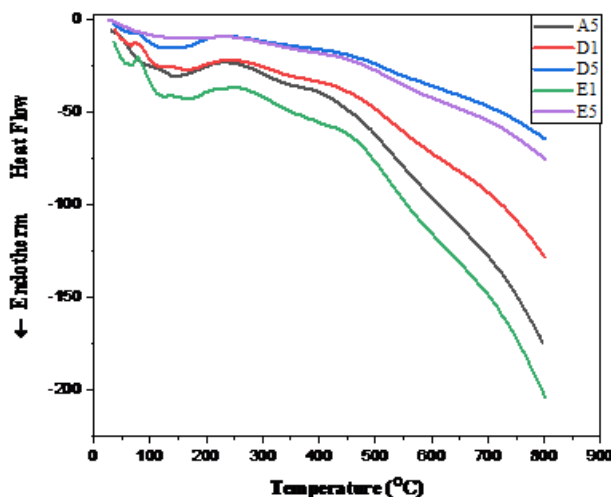


Figure 8. The DSC thermograms of Nano hybrid polymer electrolytes.

of interactions between the polymer and nanoparticles in the electrolytes [34].

4.3 Photovoltaic performance of DSSC

The highest conducting electrolytes were employed to fabricate and characterize dye-sensitized solar cell (DSSC) by sandwiching the Nano-hybrid polymer gel electrolytes. The photovoltaic parameters are exhibited in Table 3. Fig. 9 illustrates the fluctuation in J_{sc} as a consequence of the altered ionic conductivity of the Nano-hybrid polymer electrolytes. The J_{sc} outcomes exhibit exceptional concurrence with the conductivity information [35]. J_{sc} values and conductivity are positively impacted by iodide concentration. The Nano-hybrid polymer electrolytes D4 shows a decrease J_{sc} and increase V_{oc} . The decline in the J_{sc} value of this particular cell can be attributed to its reduced ionic conductivity. The ion migration resistance is elevated, leading to a reduction in the supply of I_3^- to the counter-electrode. Consequently, there is a depletion of I_3^- and a delay in the kinetics of dye regeneration, resulting in a decrease in the J_{sc} value. The E3 with 1.5 wt.% PTh displays a higher J_{sc} value, attributed to its superior ionic conductivity. This enhanced conductivity facilitates a faster regeneration process of the dye-sensitizer from its oxidized state to its original state at the dye-electrolyte interface [36–38]. The photoelectrochemical cell denoted as E3, which exhibits the highest

Table 2. The glass and melting transition phases.

Samples	T_g (°C)	T_m (°C)	H_m (J/g)	Samples Type
A5	141.52	153.21	635.3	KI
D1	66.46	140.74	317.7	$\text{SiO}_2 + \text{PTh}$
D5	65.81	137.96	191.3	
E1	67.12	144.11	175.6	MWCNTs + PTh
E5	77.54	159.75	105.3	

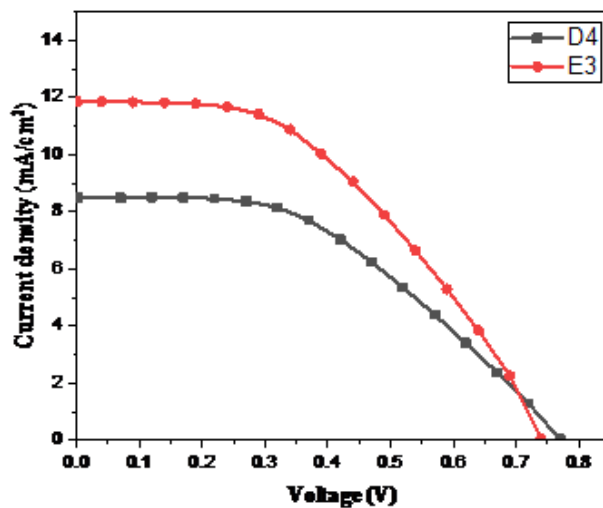


Figure 9. Photocurrent density-voltage for ITO-TiO₂/ Nano-hybrid polymer electrolytes /I₂/Pt-ITO cell.

conductivity, has demonstrated the most exceptional performance with an efficiency of 3.98%. The results of this investigation suggest that this particular system possesses highly promising characteristics that make it suitable for applications involving dye-sensitized solar cells [9]. The conduction band edge potential of Nano-TiO₂ can be positively shifted by the injection of small radius cations, like K⁺, into the lattice. This process increases the charge injection driving power, which often results in a larger J_{sc} at the expense of V_{oc} [35].

Table 3. $J - V$ performance.

Electrolytes	V_{oc} (V)	J_{sc} (mA/cm ²)	Fill Factor FF	η %
D4	0.769969	8.518005	0.450403	2.954009
E3	0.73997	11.86215	0.453669	3.982141

5. Conclusion

In this paper, Nano-hybrid polymer electrolytes are based on conductive polymer Polythiophene (PTh) by solution cast technique. The electrical conductivity was estimated between the frequencies of 50 Hz and 1 MHz and between temperatures of 293 and 343 K. The electrical conductivity change of the Nano-hybrid electrolytes was found to be dependent on the type and concentration of PTh. At room temperature, the highest conductivity values observed for the electrolyte system E3 is 11.167×10^{-2} (S/cm) for 1.5 wt.% of PTh. The real dielectric constant (ϵ_r) increased as the frequency decreased for various weight percentages of PTh. This behavior can be attributed to ion dissociation, leading to an increase in the number of available ions, while ion association causes a decrease. The blend and the Nano-hybrid electrolytes exhibit a single glass transition temperature, which indicates a high level of compatibility between

the blend components. The introduction of 2.5 weight percent of PTh particles significantly enhanced the thermal stability of the polymer blend matrix. The DSSCs with 1.5% weight percentage PTh were found to have the best photovoltaic properties, with a total conversion efficiency of 3.982%, V_{oc} of 0.74 V, J_{sc} of 11.9 mA/cm, and FF of 0.453.

Authors Contributions

Authors have contributed equally in preparing and writing the manuscript.

Availability of data and materials

Data presented in the manuscript are available via request.

Conflict of Interests

The author declare that they have no known competing financial interests or personal relationships that could have appeared to influence the work reported in this paper.

Open Access

This article is licensed under a Creative Commons Attribution 4.0 International License, which permits use, sharing, adaptation, distribution and reproduction in any medium or format, as long as you give appropriate credit to the original author(s) and the source, provide a link to the Creative Commons license, and indicate if changes were made. The images or other third party material in this article are included in the article's Creative Commons license, unless indicated otherwise in a credit line to the material. If material is not included in the article's Creative Commons license and your intended use is not permitted by statutory regulation or exceeds the permitted use, you will need to obtain permission directly from the OICC Press publisher. To view a copy of this license, visit <https://creativecommons.org/licenses/by/4.0/>.

Iraqi Journal of Physics, **19**:72–78, 2021. DOI: <https://doi.org/10.30723/ijp.v19i51.652>.

- [4] Sharma, Khushboo, V. Sharma, and S. S. Sharma. “Dye-sensitized solar cells: fundamentals and current status.”. *Nanoscale research letters*, **13**:1–46, 2018. DOI: <https://doi.org/10.1186/s11671-018-2760-6>.
- [5] H. I. Jaffer, Z. R. Al-Shammary, A. A. Abbas, and A. Qassim. “Water absorption of HDPE/Al₂O₃, TiO₂ Composites.”. *Engineering and Technology Journal*, **33**, 2015.
- [6] I. I. Nassif and B. M. Al-Shabander. “Effects of MWCNTs on the tensile properties and thermal conductivity of BaTiO₃/epoxy nanocomposites.”. *Iraqi Journal of Science*, :2226–2231, 2020. DOI: <https://doi.org/10.24996/ij.s.2020.61.9.9>.
- [7] A. R. A. Mohamed and N. Nayan. “Fabrication and analysis of dye-sensitized solar cell using natural dye extracted from dragon fruit.”. *International Journal of Integrated Engineering*, **2**, 2010. DOI: <https://doi.org/10.13140/RG.2.1.4409.1289>.
- [8] S. Rudhzhiah, A. Ahmad, I. Ahmad, and N. S. Mohamed. “Biopolymer electrolytes based on blend of kappa-carrageenan and cellulose derivatives for potential application in dye sensitized solar cell.”. *Electrochimica Acta*, **175**:162–168, 2015. DOI: <https://doi.org/10.1016/j.electacta.2015.02.153>.
- [9] S. Rudhzhiah, M. S. A. Rani, R. H. Y. Subban, A. Ahmad, N. S. Mohamed, and M. R. M. Huzaifah. “Hybrid carboxymethyl kappa-carrageenan/carboxymethyl cellulose-based biopolymer electrolytes for dye-sensitized solar cell application.”. *International Journal of Electrochemical Science*, **17**:220143, 2022. DOI: <https://doi.org/10.20964/2022.01.41>.
- [10] E. A. Swady and M. K. Jawada. “Study AC conductivity and dielectric constant of blend electrolytes.”. *AIP Conference Proceedings*, **2372**, 2021. DOI: <https://doi.org/10.1063/5.0066175>.
- [11] R. H. Almuswy and A. A. Hasan. “Electrical properties of PAN/PMMA blends doped with lithium salts.”. *Iraqi Journal of Physics*, **20**:13–28, 2022. DOI: <https://doi.org/10.30723/ijp.v20i3.1008>.
- [12] S. M. Chandra, L.-S. Chen, C.-W. Lai, Y.-H. Lee, C.-C. Chang, and C.-M. Chen. “Enhancement of power conversion efficiency of dye-sensitized solar cells for indoor applications by using a highly responsive organic dye and tailoring the thickness of photoactive layer.”. *Journal of Power Sources*, **479**:229095, 2020. DOI: <https://doi.org/10.1016/j.jpowsour.2020.229095>.
- [13] M. Nicole, M. Bonomo, L. Fagiolari, N. Barbero, C. Gerbaldi, F. Bella, and C. Barolo. “Recent advances in eco-friendly and cost-effective materials towards sustainable dye-sensitized solar cells.

- ”. *Green chemistry*, **22**:7168–7218, 2020. DOI: <https://doi.org/10.1039/D0GC01148G>.
- [14] A. M. Shakeel, A. K. Pandey, and N. Abd Rahim. “Advancements in the development of TiO₂ photoanodes and its fabrication methods for dye sensitized solar cell (DSSC) applications. A review.”. *Renewable and Sustainable Energy Reviews*, **77**:89–108, 2017. DOI: <https://doi.org/10.1016/j.rser.2017.03.129>.
- [15] A. Parbin. “The fabrication of a highly conductive ceria-embedded gadolinium-stabilized bismuth oxide nanocomposite solid electrolyte for low-temperature solid oxide fuel cells.”. *Materials Advances*, **3**:3316–3325, 2022. DOI: <https://doi.org/10.1039/D1MA01254A>.
- [16] S. S. Salehan, B. N. Nadirah, M. S. M. Saheed, W. Z. N. Yahya, and M. F. Shukur. “Conductivity, structural and thermal properties of corn starch-lithium iodide nanocomposite polymer electrolyte incorporated with Al₂O₃.”. *Journal of Polymer Research*, **28**: 1–11, 2021. DOI: <https://doi.org/10.1007/s10965-021-02586-y>.
- [17] S. Kumar, V. S. Manikandan, S. K. Panda, S. P. Senanayak, and A. K. Palai. “Probing synergistic outcome of graphene derivatives in solid-state polymer electrolyte and Pt-free counter electrode on photovoltaic performances.”. *Solar Energy*, **208**:949–956, 2020. DOI: <https://doi.org/10.1016/j.solener.2020.08.060>.
- [18] S. Idayu, A. Halim, C. H. Chan, and J. Apotheker. “Basics of teaching electrochemical impedance spectroscopy of electrolytes for ion-rechargeable batteries—part 1: a good practice on estimation of bulk resistance of solid polymer electrolytes.”. *Chemistry Teacher International*, **3**:105–115, 2021. DOI: <https://doi.org/10.1515/cti-2020-0011>.
- [19] S. M. Abdelcareem and M. K. Jawad. “Investigate salts type and concentration on the conductivity of polymer electrolyte.”. *Iraqi Journal of Physics*, **17**:42–50, 2019. DOI: <https://doi.org/10.30723/ijp.v17i42.437>.
- [20] A. S. Mohamed, A. S. F. M. Asnawi, M. F. Shukur, J. Matmin, M. F. Z. Kadir, and Y. M. Yusof. “The development of chitosan-maltodextrin polymer electrolyte with the addition of ionic liquid for electrochemical double layer capacitor (EDLC) application.”. *International Journal of Electrochemical Science*, **17**, 2022. DOI: <https://doi.org/10.20964/2022.03.30>.
- [21] E. A. Swady and M. K. Jawad. “Dependency of the AC conductivity of blend nanocomposites on the LiI and ZnO percent.”. *AIP Conference Proceedings*, **2437**:020053, 2022. DOI: <https://doi.org/10.1063/5.0092661>.
- [22] A. Arya and A. L. Sharma. “Temperature and salt-dependent dielectric properties of blend solid polymer electrolyte complexed with LiBOB.”. *Macromolecular Research*, **27**:334–345, 2019. DOI: <https://doi.org/10.1007/s13233-019-7077-5>.
- [23] S. B. Aziz, T. J. Woo, M. F. Z. Kadir, and H. M. Ahmed. “A conceptual review on polymer electrolytes and ion transport models.”. *Journal of Science: Advanced Materials and Devices*, **3**:1–17, 2018. DOI: <https://doi.org/10.1016/j.jsamd.2018.01.002>.
- [24] J. Silva, S. Lanceros-Mendez, and R. Simões. “Effect of cylindrical filler aggregation on the electrical conductivity of composites.”. *Physics Letters A*, **378**:2985–2988, 2014. DOI: <https://doi.org/10.1016/j.physleta.2014.08.011>.
- [25] Y. Zare. “Study of nanoparticles aggregation/agglomeration in polymer particulate nanocomposites by mechanical properties.”. *Composites Part A: Applied Science and Manufacturing*, **84**:158–164, 2016. DOI: <https://doi.org/10.1016/j.compositesa.2016.01.020>.
- [26] M. A. Morsi, A. Rajeh, and A. A. Al-Muntaser. “Reinforcement of the optical, thermal and electrical properties of PEO based on MWCNTs/Au hybrid fillers: nanodielectric materials for organoelectronic devices.”. *Composites Part B: Engineering*, **173**:106957, 2019. DOI: <https://doi.org/10.1016/j.compositesb.2019.106957>.
- [27] A. H. Bushra and H. H. Issa. “Dielectric properties and AC electrical conductivity analysis of (La₂O₃)_{1-x} (ZnO)_x.”. *IOP Conference Series: Materials Science and Engineering*, **928**:072003, 2020. DOI: <https://doi.org/10.1088/1757-899X/928/7/072003>.
- [28] M. Irfan, A. Manjunath, S. S. Mahesh, R. Somashekar, and T. Demappa. “Influence of NaF salt doping on electrical and optical properties of PVA/PVP polymer blend electrolyte films for battery application.”. *Journal of Materials Science: Materials in Electronics*, **32**:5520–5537, 2021. DOI: <https://doi.org/10.1007/s10854-021-05274-1>.
- [29] F. M. Ahmed and M. K. Jawad. “FTIR and electrical behavior of blend electrolytes based on (PVA/PVP).”. *Iraqi Journal of Physics*, **21**:1–9, 2023. DOI: <https://doi.org/10.30723/ijp.v21i1.1093>.
- [30] F. M. Ahmed and M. K. Jawad. “Characterization of blend electrolytes containing organic and inorganic nanoparticles.”. *Polymer*, **7**:8, 2024.
- [31] P. Manafi, H. Nazockdast, M. Karimi, M. Sadighi, and L. Magagnin. “A study on the microstructural development of gel polymer electrolytes and different imidazolium-based ionic liquids for dye-sensitized solar cells.”. *Journal of Power Sources*, **481**:228622, 2021. DOI: <https://doi.org/10.1016/j.jpowsour.2020.228622>.

- [32] M. K. Abid, M. M. Abbas, N. K. Abid, and M. K. Jwad. “Investigate the thermal analysis properties of polymer electrolyte.”. *Journal of Physics: Conference Series*, **2114**:012048, 2021. DOI: <https://doi.org/10.1088/1742-6596/2114/1/012048>.
- [33] D. Golodnitsky, E. Strauss, E. Peled, and S. Greenbaum. “On order and disorder in polymer electrolytes.”. *Journal of The Electrochemical Society*, **162**:A2551, 2015. DOI: <https://doi.org/10.1149/2.0161514jes>.
- [34] M. T. Ramesan, P. Jayakrishnan, T. Anilkumar, and G. Mathew. “Influence of copper sulphide nanoparticles on the structural, mechanical and dielectric properties of poly (vinyl alcohol)/poly (vinyl pyrrolidone) blend nanocomposites.”. *Journal of Materials Science: Materials in Electronics*, **29**:1992–2000, 2018. DOI: <https://doi.org/10.1007/s10854-017-8110-0>.
- [35] M. K. Jawad. “Polymer electrolytes based PAN for dye-sensitized solar cells.”. *Iraqi Journal of Physics*, **33**:143–150, 2017. DOI: <https://doi.org/10.30723/ijp.v15i33.150>.
- [36] N. A. Dzulkurnain, A. R. Mohd Saiful, A. Azizan Ahmad, and M. Nor Sabirin. “Effect of lithium salt on physicochemical properties of P (MMA-co-EMA) based copolymer electrolytes for dye-sensitized solar cell application.”. *Ionics*, **24**:269–276, 2018. DOI: <https://doi.org/10.1007/s11581-017-2190-y>.
- [37] M. Y. A. Rahman, A. Ahmad, A. A. Umar, R. Taslim, M. S. Su’ait, and M. Salleh. “Polymer electrolyte for photoelectrochemical cell and dye-sensitized solar cell: a brief review.”. *Ionics*, **20**:1201–1205, 2014. DOI: <https://doi.org/10.1007/s11581-014-1211-3>.
- [38] R. M. Saiful Asmal, N. A. Abdullah, M. H. Sainorudin, M. Masita, and S. Ibrahim. “The development of poly (ethylene oxide) reinforced with a nanocellulose-based nanocomposite polymer electrolyte in dye-sensitized solar cells.”. *Materials Advances*, **2**:5465–5470, 2021. DOI: <https://doi.org/10.1039/D1MA00206F>.